

See discussions, stats, and author profiles for this publication at: <https://www.researchgate.net/publication/345391213>

Combining disciplines: Dealing with observed and cryptic animal residencies in passive telemetry data by applying econometric decision-making models

Article in *Ecological Modelling* · November 2020

DOI: 10.1016/j.ecolmodel.2020.109340

CITATIONS

0

READS

53

7 authors, including:



Stijn Bruneel
Ghent University

15 PUBLICATIONS 86 CITATIONS

[SEE PROFILE](#)



Pieterjan Verhelst
Ghent University

20 PUBLICATIONS 143 CITATIONS

[SEE PROFILE](#)



Jan Reubens
Vlaams Instituut Voor De Zee

47 PUBLICATIONS 606 CITATIONS

[SEE PROFILE](#)



Stijn Luca
Ghent University

32 PUBLICATIONS 187 CITATIONS

[SEE PROFILE](#)

Some of the authors of this publication are also working on these related projects:



HEART: HEalth related Activity Recognition system based on IoT [View project](#)



CROSSLINK [View project](#)

Combining disciplines: dealing with observed and cryptic animal residencies in passive telemetry data by applying econometric decision-making models

Stijn Bruneel^{1,2*}, Pieterjan Verhelst², Jan Reubens³, Stijn Luca⁴, Johan Coeck⁵, Tom Moens², Peter Goethals¹

¹*Department of Animal Sciences and Aquatic Ecology, Ghent University, Coupure Links 653, 9000 Ghent, Belgium,*

²*Marine Biology Research Group, Ghent University, Krijgslaan 281, 9000 Ghent, Belgium,*

³*Flanders Marine Institute (VLIZ), Wandelaarkaai 7, 8400 Ostend, Belgium,*

⁴*Department of Data Analysis and Mathematical Modelling, Ghent University, Coupure Links 653, 9000 Ghent, Belgium,*

⁵*Research Institute for Nature and Forest (INBO), Havenlaan 88, bus 73, 1000 Brussels, Belgium,*

** To whom correspondence should be addressed; E-mail: stijn.bruneel@ugent.be*

Abstract

Migratory species do not necessarily behave migratory continuously. An important aspect of studying migratory species is therefore to distinguish between movement and resident behaviour. Telemetry is a rapidly evolving technique to study animal movement, but the number of data processing techniques to account for resident behaviour remains limited. In this study we describe how models that were initially developed to predict human customer behavior, i.e. two-part and three-part models, provide new insights in the movement of migrating eel by accounting for resident behaviour apparent from telemetry data sets. In econometrics, two-part models take into account that the decision of a customer to purchase an item and the deci-

sion of the customer on the purchase quantity of the concerning product, might be affected by different factors. Similarly, the decision of a fish to migrate or to stay resident might be affected by different factors than the decision of the fish to swim fast or slow. Telemetry data of eel movement in the Permanent Belgian Acoustic Receiver Network (PBARN) of the Scheldt Estuary was used. This network with high detection probabilities allowed residencies to be recognized, defined, and introduced as zero values in a movement-residency data set. Two-part models, which consider movement decision, i.e. residency or movement, and movement intensity, i.e. swimming speed, as two different processes or parts of one larger model, outperformed one-part models that do not make that distinction. This underlines the complex migration behaviour eels exhibit. These two-part models in turn were outperformed by three-part models that also accounted for cryptic (i.e. unobserved) residencies. While the one-part model identified the tides and the distance from the most upstream gate as most important for movement, the three-part models identified the tides as most important for the movement decision and the distance from the most upstream gate as most important for the movement intensity. Considering movement decisions, cryptic residencies and movement intensity in modelling efforts increased model performance by 9.8 %, underlining the importance of acknowledging the potentially complex behaviour animals exhibit.

Keywords: Acoustic telemetry, Fish movement, Residencies, Gates, Two-part and three-part models, Eel migration

1 **1. Introduction**

2 Zero values are often encountered in ecological count data where they
3 typically represent absences. However, zeros may have different meanings
4 as they may arise from real absences due to habitat unsuitability, or from
5 false absences due to observer and design errors ([Blasco-Moreno et al., 2019](#)).
6 Similarly, in telemetry studies, data-sets can be heavily zero-inflated if mo-
7 ments of non-detection are considered as zeros ([Brownscombe et al., 2019](#);
8 [Whoriskey et al., 2019](#)), with the meaningfulness of these zeros being strongly
9 dependent on the network design ([Bruneel et al., 2020](#)). Since the objective
10 of many telemetry studies is to describe movement behaviour of animals, zero
11 values could be used as an indication of non-movement or residency. How-
12 ever, accounting for resident behavior, represented as zero values in telemetry
13 data, might require adapted models. Therefore, the aim of this study is to
14 evaluate currently used models and to assess the potential of alternative
15 models to deal with such data.

16 A good network design is key to define zero values. In estuarine and
17 riverine acoustic networks with good detection probabilities, receivers may
18 act as gates that tagged animals need to pass to leave a specific area ([Kraus
19 et al., 2018](#); [Steckenreuter et al., 2017](#)). Therefore, animals which remain
20 undetected could still be positioned within a zone of the study area, i.e.
21 between two gates, allowing periods of non-detection to be considered as
22 residencies between detections ([Bruneel et al., 2020](#)).

23 However, the specific animal behaviour between detections remains often

24 entirely unknown, unless some expert-knowledge, such as typical swimming
25 speed and spawning period, is integrated. For example, a fish known to
26 migrate during a certain period would be expected to perform highly uni-
27 directional movement behavior and unexpected travel delays would be an
28 indirect indication of resident behavior between detections. Since these resi-
29 dencies between detections cannot be observed directly, they are referred to
30 as cryptic residencies.

31 Zero-inflated data sets often require adapted statistical tools. Depend-
32 ing on the nature of zeros, different statistical ecological models have been
33 suggested. If both false and true zeros are likely to be present, zero in-
34 flated models are typically used, while hurdle models are used when there
35 are only true zeros (Zuur et al., 2009). More specifically, hurdle models as-
36 sume that two processes result in two distinct signals, i.e. zero versus not
37 zero, while zero-inflated models assume that both processes can yield zero
38 values. For example, in case detection probabilities are low, individual fish
39 not being detected might actually be present, yielding false zeros in addi-
40 tion to structural zeros. In such a case, zero-inflated models would be most
41 appropriate. Within the field of ecology, zero-inflated and hurdle models
42 typically refer to models able to deal with count data inflated with observed
43 absences (Blasco-Moreno et al., 2019; Joseph et al., 2009; Zuur et al., 2009).
44 Although continuous and proportional ecological data sets are omnipresent,
45 model equivalents for these types of data are not often used. However, for
46 continuous ecological data, such as fish swimming speed, models with a sim-

47 ilar approach but different underlying distribution could be useful. More
48 specifically, for count data, Poisson or negative binomial distributions are
49 typically used, while for continuous data, Gaussian or Gamma distributions
50 would be more appropriate. In econometric studies for example, the contin-
51 uous equivalents of hurdle models, known as two-part models, have already
52 been used frequently (Deb and Holmes, 2002; Farewell et al., 2017).

53 Excess zeros are often considered a nuisance as they typically require
54 more complex models with more parameters to be defined (Warton, 2005).
55 However, explicitly accounting for zero-values may be useful as they may
56 represent a unique signal of an unconsidered process. For example, in econo-
57 metrics, two-part models have been widely used to study customer behaviour
58 (Neelon et al., 2016; Pohlmeier and Ulrich, 1995). A customer might decide
59 to purchase a product (Will I buy this?), but after that decision he/she would
60 also need to decide on the quantity of the product (How much of it will I
61 buy?). The conditions that drive the customer to purchase may be differ-
62 ent from those driving the level of consumption. Hence, accounting for each
63 process separately may be necessary to understand customer behavior.

64 Similarly, the factors that trigger fish movement, i.e. the movement de-
65 cision, may be different from the factors determining the distance or speed
66 with which the fish moves, i.e. the movement intensity. Hence, accounting for
67 movement decision and intensity separately may also be necessary to under-
68 stand fish movement behavior. Therefore, the aim of this study was to assess
69 the added value for predictions and the implications for ecological knowledge

70 of distinguishing between both processes of fish movement behavior. More
71 specifically, we compared the predictive performance and inferred ecological
72 knowledge of one-part and two-part models describing the movement be-
73 haviour of migrating eel (*Anguilla anguilla* L.) in the Scheldt Estuary. In
74 addition, to assess whether a further compartmentalization (e.g. distinction
75 between upstream and downstream movement) would provide added value,
76 different three-part models were constructed and compared with the one-part
77 and two-part models.

78 Given the increasing data availability and complexity entailed by the ex-
79 ponential increase of possible associations among predictors, machine learn-
80 ing is gaining ground among movement ecologists because of its high predic-
81 tive performance and alleged ease of use (Wang, 2019; Joseph et al., 2017).
82 However, although machine learning is built on a statistical framework, the
83 outputs of pattern-learning algorithms are often difficult to interpret in the
84 wider context of system functioning (Bzdok et al., 2018). Therefore, in prac-
85 tice, the choice between machine learning and statistical models is typically
86 determined by the purpose, which is either to make predictions or to infer
87 knowledge, respectively. However, since ecologists typically want the best of
88 both worlds, i.e. a model that is interpretable in terms of ecological knowl-
89 edge while remaining broadly applicable for predictions, statistical models
90 and machine learning should be treated as complementary tools. Therefore,
91 we also compared the interpretability and the predictive performance of sta-
92 tistical models (i.e. one-part and two-part regression models), hybrid models

93 (i.e. three-part models that combine neural networks with generalized lin-
94 ear regression) and machine learning algorithms (i.e. conditional inference
95 random forests (RF)) for the current telemetry data set.

96 **2. Materials and methods**

97 *2.1. Study area*

98 The Schelde Estuary is a well-mixed estuary of 160 km long without
99 transversal man-made migration barriers and characterized by strong cur-
100 rents, high turbidity and a large tidal amplitude up to 6 m (Cornet et al.,
101 2016). The estuary can be divided in two regions (upstream to downstream):
102 the Zeeschelde, which spans 105 km from Ghent to Antwerp (Belgium), and
103 the Westerschelde, which covers the 55 km from Antwerp to the mouth of
104 the estuary at Vlissingen (The Netherlands). The width of the Zeeschelde
105 varies between 50 to 1350 m while the width of the Westerschelde varies
106 between 2000 and 8000 m (Fig. 1). The description of the study area was
107 adopted from Bruneel et al. (2020). This study was limited to the part of the
108 Zeeschelde, because of the relatively low detection probability of the gates in
109 the Westerschelde (see section 2.3).

110 *2.2. Tagging procedure*

111 At the tidal weir in Merelbeke (Ghent), 100 eels were caught and inter-
112 nally tagged with V13 (VEMCO Ltd., Canada) coded acoustic transmitters
113 (Verhelst et al., 2018). After capture, surgery and recovery (Thorstad et al.,

114 2013), fish were released at the nearest receiver. Of the 100 tagged eels, 58
115 migrated. The migration period of these 58 eels was determined (Verhelst
116 et al., 2018) and used for further analysis. A more detailed description of the
117 tagging procedure is provided in Appendix A. The description of the tagging
118 procedure was adopted from Bruneel et al. (2020).

119 2.3. Acoustic network

120 Within the framework of the Belgian LifeWatch observatory, a permanent
121 longitudinal network of receivers (VR2W, VEMCO Ltd, Canada) has been
122 deployed since the spring of 2014 in the Schelde Estuary (Reubens et al.,
123 2019a). Currently, the network consists of 25 receivers, deployed from the
124 river bank, which were combined into 18 gates and are on average 4969 m
125 apart (Fig. 1 and Table B.1). At four locations (s15, s16, s17 and s18), a
126 receiver on each side of the estuary was deployed to cover the whole width.
127 The exact detection range for the different receivers in the Zeeschelde was
128 unknown, but ranges between 300 m and 1000 m (Verhelst et al., 2018). Re-
129 sults from the network in the North Sea suggest that it is strongly dependent
130 on current velocity and wave action and will therefore be characterized by
131 a strong spatial and temporal variability (Reubens et al., 2019b). The de-
132 tection probability of the gates was estimated using the conditional nature
133 of fish movement throughout the system (Brownscombe et al., 2019). Since
134 there are no other pathways to the North Sea, tagged fish have to pass the
135 different gates in a well-defined order and detection probability can be defined

136 as the probability of detecting a tag moving past a specific gate (Melnichuk,
 137 2012; Perry et al., 2012). The detection probabilities of the different gates
 138 are given in Table B.1. The description of the acoustic network was adopted
 139 from Bruneel et al. (2020).

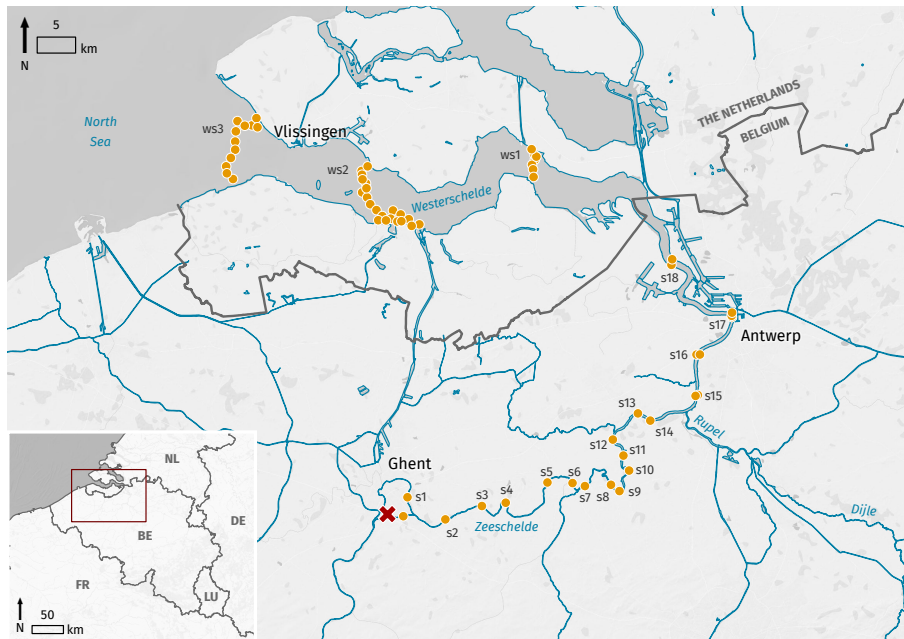


Figure 1: The Schelde Estuary comprises the Zeeschelde (Ghent-Antwerp) and Westerschelde (Antwerp-Vlissingen). The receivers are represented as orange circles. The gates are indicated as labels for different groups of receivers. The weir in Ghent where the eels were caught and released is depicted as a red cross. Detections at the three gates in the Westerschelde (ws1, ws2 and ws3) were not considered in this study because of their relatively low detection probabilities. Adapted from Bruneel et al. (2020).

140 2.4. Eel movement

141 Given the high average detection probability of 97.0 % in the Zeeschelde,
 142 the number of false zeros was likely limited. In addition, since the movement
 143 of eels is highly unidirectional once they have started migrating, eels not

144 being detected at one gate are likely to be detected at the next gate, causing
145 some reduction in resolution, but still providing a reliable position estimate.
146 Since false zeros, due to low detection probabilities, are unlikely, we decided
147 to work with two-part models instead of zero-inflated models.

148 When a tagged eel was consecutively detected at two different gates,
149 we considered the time lapse between these two detections as a movement
150 interval and the distance between the two gates was determined. When
151 a tagged eel was detected multiple times at a specific gate without being
152 detected at any other gate, the time lapse between the earliest and last
153 detection was considered as a residency interval and was assigned a distance
154 value of zero. It should be noted that some short intervals might actually have
155 been identified incorrectly as residency intervals. For example, a migrating
156 eel might come within the detection range and have multiple detections while
157 moving from one side of the gate to the other. Although considered as
158 highly variable in literature ([Breukelaar et al., 2009](#); [Verbiest et al., 2012](#)),
159 we assumed an average migration speed of 0.25 m s^{-1} and a detection range
160 of 250 meter, yielding an approximate threshold value of at least 30 minutes
161 for residency intervals. To ensure that movement was not wrongly identified
162 as residencies, this value was doubled and all residency intervals with a time
163 span below 1 hour were omitted from the analysis (10.80 % of the residency
164 intervals were retained for analysis).

165 It is possible that, before heading to the next gate, a tagged eel was
166 resident between two gates without entering either gate's detection range.

167 Such unobserved or cryptic residencies are not directly apparent from the
168 data as they are observed as being part of the movement interval. However,
169 these cryptic residencies can be accounted for indirectly as they will cause a
170 travel delay in the movement interval, negatively affecting the time necessary
171 to reach the next gate.

172 Recognizing resident behavior in acoustic telemetry networks based on
173 position estimates alone often remains a difficult objective (Cagua et al.,
174 2015). In this specific study, indirect (i.e. through travel delays) and di-
175 rect indications of apparent non-movement can be either the result of (i) fish
176 choosing to be resident and to discontinue swimming or (ii) fish swimming
177 against the currents without much net gain in distance covered. However, if
178 there are clear signs of individual variation and enough individuals to account
179 for it, a distinction between both can be made. When animals are resident,
180 they cannot be distinguished from each other using position estimates alone.
181 However, when they migrate, even against the current, the strongest and
182 fastest individuals will reach higher swimming speeds and can as such be
183 distinguished from weaker and slower individuals. It should be noted that
184 throughout the manuscript, swimming speed represents the ground speed
185 (i.e. geographical progress per unit of time) without correction for current
186 speed. As each tag emits a signal at a unique frequency, individuals can be
187 identified and individual variation in swimming speed can be determined and
188 used to analyse the behavior associated with apparent non-movement. Since
189 European eel and other migrating fish have been found to apply different

190 strategies to save energy, it is much more likely that eels would choose the
191 most energy efficient option and choose to be resident when facing currents
192 rather than to swim without much net gain in distance covered ([Arnold and](#)
193 [Cook, 1984](#); [Glebe and Leggett, 1981](#); [Metcalf et al., 1990](#)). Therefore, we
194 consider measurements of apparent non-movement as residencies and eval-
195 uate afterwards whether this choice was justified based on the outcomes of
196 the models.

197 To normalize the data, distances were divided by time, yielding swimming
198 speed. Residency and movement intervals with a time lapse higher than
199 one full tidal cycle were removed (13.42 % data removal) as they do not
200 allow to contribute movement behaviour to either ebb tide, flood tide or a
201 combination of both (see section [2.5](#)). To account for telemetry detection
202 errors that might cause unrealistic swimming speeds, movement intervals
203 with a swimming speed of 1.5 interquartile ranges (IQRs) below the first
204 quartile or above the third quartile were considered outliers and removed
205 from the data set ([Tukey, 1977](#)). In practice, all movement intervals with a
206 swimming speed higher than 2.7 or lower than -1.5 m/s were omitted from
207 the analysis (additional 2.20 % data removal). In summary, first 89.20 % of
208 residency intervals were removed, followed by a 13.42 % removal from the
209 entire data set (movement intervals + residency intervals), followed by a 2.20
210 % removal from the entire data set. The final data set contained 19.24 and
211 80.76 % residency and movement intervals, respectively.

212 *2.5. Environmental data*

213 As the biological response in this study was analysed at a relatively fine
214 spatiotemporal resolution (Bultel et al., 2014; Verhelst et al., 2018), a sound
215 coupling of biological and environmental data would have been challenging
216 and use of daily averages would have yielded inconclusive results on within-
217 day movement patterns. Therefore only variables were included that were
218 fixed in time (i.e. distance from source), fixed in space (i.e. day phase),
219 known to be accurate at high spatial and temporal resolutions (i.e. period
220 of flooding and period of ebbing), or known to be well represented by daily
221 averages (i.e. moon and tidal phase). It should be noted that the main
222 aim of this study was to assess the potential of alternative ecological models
223 rather than to identify all environmental factors affecting eel migration. To
224 obtain a more comprehensive understanding of these environmental factors,
225 more fine-scale measurements and/or simulations of potentially important
226 environmental variables, such as discharge, temperature, salinity and precip-
227 itation could be used to fine-tune the developed models.

228 To account for the distances between the locations of the gates and of the
229 tidal measuring stations, a weighted average method was applied to estimate
230 the precise moments of low and high water at the gates. The closest upstream
231 and downstream tidal measuring stations were assigned to each gate. Based
232 on the distances between these tidal stations and the gate, linear weights were
233 assigned to both tidal stations. When tidal data at the respective upstream or
234 downstream tidal station was absent or of questionable quality (e.g. outliers

235 and known periods of malfunctioning measuring devices) at the time interval
236 of interest, the next upstream or downstream tidal station was chosen. This
237 allowed us to estimate the duration of ebbing and flooding for each movement
238 and residency interval. The ratio of period flood tide (minutes) over total
239 period of the interval (minutes) was determined and used as a predictor, i.e.
240 flood ratio. Per gate, the ratio of the maximum difference in water level of
241 the concerning day over the median of the maximum difference in water level
242 per day of the entire study period was used as a proxy for tidal phase, with
243 low values being associated with neap tide and large values with spring tide.
244 Moon phase was a numerical value representing the degree of illumination of
245 the moon, ranging from new moon (0) to full moon (1). Time of day was a
246 categorical variable with the classes Day, Night, Dusk and Dawn. Distance
247 from source gave the distance (km) from the most upstream gate to the
248 detecting gate.

249 *2.6. Model construction and evaluation*

250 All analyses were performed using the R software (version 3.6.2, R Devel-
251 oper Core Team, R Foundation for Statistical Computing, Vienna, Austria).
252 To construct the different models, the *stats*, *nnet* and *ranger* packages were
253 used.

254 *2.6.1. Model construction*

255 In the one-part, two-part, three-part and random forest models, swim-
256 ming speed was used as response variable, while flood ratio, tidal phase,

257 moon phase, day phase and distance from source were evaluated as potential
 258 predictors. Linear weights were introduced in model construction and eval-
 259 uation to account for the different number of observations between eels. As
 260 a consequence each eel contributed equally to the constructed models. First,
 261 a one-part model was constructed for the entire data set which consisted of
 262 a multiple linear regression model with Gaussian distribution.

263 Second, continuous two-part models were constructed which consisted
 264 of two sub-models (Belotti et al., 2015; Humphreys, 2013): (1) A binomial
 265 model for the entire data set, with movement and residency as contrasts,

$$Pr(y \neq 0|\mathbf{x}) = F(\mathbf{x}^T \boldsymbol{\alpha}) \tag{1}$$

266 where y is the response variable, \mathbf{x} is a vector of predictors ($\mathbf{x} = (1, x_1, \dots, x_k)$,
 267 with k the number of predictors), $\boldsymbol{\alpha}$ is the corresponding vector of parameters
 268 to be estimated ($\boldsymbol{\alpha} = (\alpha_0, \alpha_1, \dots, \alpha_k)$, with k the number of parameters), and
 269 F is the cumulative distribution function of an independent and identically
 270 distributed error term from a probit model. (2) A multiple linear model with
 271 Gaussian distribution solely for the movement data,

$$\theta(y|y \neq 0, \mathbf{x}) = h(\mathbf{x}^T \boldsymbol{\beta}) \tag{2}$$

272 where θ is the probability density function, $\boldsymbol{\beta}$ is the corresponding vector of
 273 parameters to be estimated, and h is a Gaussian density function for y with
 274 expectation $x^T \boldsymbol{\beta}$ and some constant variance σ^2 . The likelihood contribution

275 for an observation can be written as,

$$\theta(y) = \{1 - F(\mathbf{x}^T \boldsymbol{\alpha})\}^{i(y=0)} \times \{F(\mathbf{x}^T \boldsymbol{\alpha})h(\mathbf{x}^T \boldsymbol{\beta})\}^{i(y \neq 0)} \quad (3)$$

276 where $i(\cdot)$ denotes the indicator function. Then, the log-likelihood contribu-
277 tion is,

$$\ln(\theta(y)) = i(y = 0)\ln \{1 - F(\mathbf{x}^T \boldsymbol{\alpha})\} + i(y \neq 0)[\ln \{F(\mathbf{x}^T \boldsymbol{\alpha})\} + \ln \{h(\mathbf{x}^T \boldsymbol{\beta})\}] \quad (4)$$

278 Because the $\boldsymbol{\alpha}$ and $\boldsymbol{\beta}$ parameters are additively separable in the log-likelihood
279 contribution for each observation, the models for the full data set and the non-
280 zeros can be estimated separately. Predictions of y_i , $\hat{y}_i|x_i$, were obtained by
281 multiplying the predictions from each part of the model for the corresponding
282 observations,

$$\hat{y}_i|x_i = (\hat{p}_i|\mathbf{x}_i) \times (\hat{y}_i|y_i \neq 0, \mathbf{x}_i) \quad (5)$$

283 where $\hat{p}_i|\mathbf{x}_i$ is the predicted probability that $y_i \neq 0$. To obtain the most
284 parsimonious model, each part of the model was constructed using a step-
285 wise approach with AIC as selection criteria,

$$AIC = -2\ln L + 2k \quad (6)$$

286 where L is the maximum value of the likelihood function and k the number
287 of estimated parameters.

288 By definition, two-part models assume that both parts of the model are
289 independent. However, this should not always necessarily be the case. There-
290 fore, the added value of accounting for any dependence between both parts
291 was also assessed. This type of models are referred to as selection models in
292 literature, and can be constructed using a two-stage estimation procedure:
293 (1) The Inverse Mills Ratio (IMR) is determined from the binomial model
294 for the full data set, and (2) the linear regression model for the movement
295 data is constructed with IMR as additional covariate (Heckman, 1979). The
296 IMR is,

$$IMR(\mathbf{x}) = \frac{\phi(\mathbf{x})}{\Phi(\mathbf{x})} \quad (7)$$

297 with ϕ the standard normal density, Φ the standard normal cumulative dis-
298 tribution function and \mathbf{x} the vector of linear predictors of the binomial model.

299 To assess whether further distinction between upstream and downstream
300 movement would improve the predictions, a three-part model was constructed.
301 This model consisted of 1) a multinomial model (via neural networks) with
302 three contrasts: residency, upstream movement and downstream movement;
303 2) a linear model of the upstream movement; and 3) a linear model of the
304 downstream movement.

305 One could argue that the few upstream intervals (3.7 % of the total
306 amount of intervals per eel), actually represented residency intervals gone
307 wrong (i.e. eel trying to stay resident are in fact slightly pushed back up-
308 stream; see also section 3.1). Therefore additional one-part and two-part

309 models were constructed after transformation of the few upstream movement
310 intervals into residency intervals, i.e. they were given a value 0.

311 Additionally, a three-part model was constructed as an attempt to ac-
312 count for the bimodal pattern of the data (See section 3.1). The three parts
313 in this model were: 0 vs 0 to threshold vs threshold to 2.7 m s^{-1} . After assess-
314 ing the predictive performance of models with different thresholds (threshold
315 interval selection based on inspection of stacked density plots in section 3.1)
316 from 0.3 to 0.7 with a step-size of 0.01 and 10^4 Monte-Carlo cross-validations,
317 the threshold that yielded the model with the highest predictive performance
318 was retained (threshold = 0.45 m s^{-1} ; see section 3.2).

319 Finally, conditional inference random forests were used to analyse both
320 data sets, i.e. with and without upstream movement intervals. Different
321 parameter settings were assessed, but since default parameters gave slightly
322 higher performances, only these results were reported.

323 *2.6.2. Model performance*

324 To assess the performance of the models, Monte Carlo cross-validations
325 were performed with 10^6 repeats, during which some individuals were used
326 for training and some for testing. Different ratios (2/3, 3/4, 4/5, 5/6, 6/7,
327 7/8, 8/9 and 9/10 for training) were assessed but since very similar results
328 were obtained within each model, e.g. 0.1 % difference in Root Mean Square
329 Error (RMSE), only results for a ratio of 9/10-1/10 for training-testing, were
330 reported. Per repeat, a step-wise approach with AIC as selection criterion

331 was used to arrive at the most parsimonious model. Per repeat the RMSE
332 was calculated as given in Eq. 8, with m the number of eels in the test data
333 set, n_k the number of observations of eel k , y_j the actual value and $\hat{y}_j|x_j$ the
334 predicted value of the swimming speed. Finally, the average RMSE over all
335 repeats was determined.

$$RMSE = \frac{1}{m} \sum_{k=1}^m \sqrt{\frac{1}{n_k} \sum_{j=1}^{n_k} (y_j - \hat{y}_j|x_j)^2} \quad (8)$$

336 2.6.3. Model validation

337 To quantify the uncertainty of the parameter estimates, bootstrap confi-
338 dence intervals were determined. While standard parametric inferences rely
339 on a-priori assumptions of the underlying distribution of the population, the
340 non-parametric resampling approach of bootstrapping provides an estimate
341 of the statistic's sampling distribution using within-sample variation. More
342 specifically, by considering the sample distribution as representative for the
343 population distribution, bootstrapping can be used to estimate the quality of
344 the predictive model. First, to develop the most parsimonious models, model
345 selection was performed using the procedure described by [Austin and Tu](#)
346 [\(2004\)](#), based on bootstrap samples, backwards elimination and AIC ($n=10^4$).
347 Second, the coefficient estimates of the retained variables and their 95% boot-
348 strap percentile confidence intervals were determined ($n=10^4$) ([Davison and](#)
349 [Hinkley, 1997](#)). Linear bootstrap sampling weights were used to account for
350 the different number of observations between eels.

351 *2.6.4. Extension to one-part and two-part mixed models*

352 One major advantage of telemetry is its ability to provide data on the
353 level of individuals and therefore mixed models that account for individual
354 correlation are commonly used. Therefore, we also compared the explanatory
355 power of one-part mixed models and two-part mixed models. Both models
356 had eel ID as random intercept. The RMSE values were used as proxies
357 of explanatory power. Since in the two-part models independence between
358 parts is assumed, we did not account for any correlation across both fixed
359 effects and random effects from the different parts of the two-part model (i.e.
360 the random effects of the binomial model and those of the linear model were
361 determined independently).

362 **3. Results**

363 *3.1. Exploratory analysis*

364 An exploratory analysis of the data suggests that downstream movement
365 intervals generally took place during ebb tide (Figs 2 and C.1). The nor-
366 malized duration of flood tide in the downstream movement intervals was
367 either 0 or to a lesser extent 100 % (Fig. 2), suggesting that downstream
368 movement intervals contained either no flooding at all or a full flood cycle.
369 On the other hand, upstream movement intervals typically took place during
370 flood tide (Figs 2 and C.1). Finally, residencies seemed to occur more often
371 during flood tide than during ebb tide (Fig. 2).

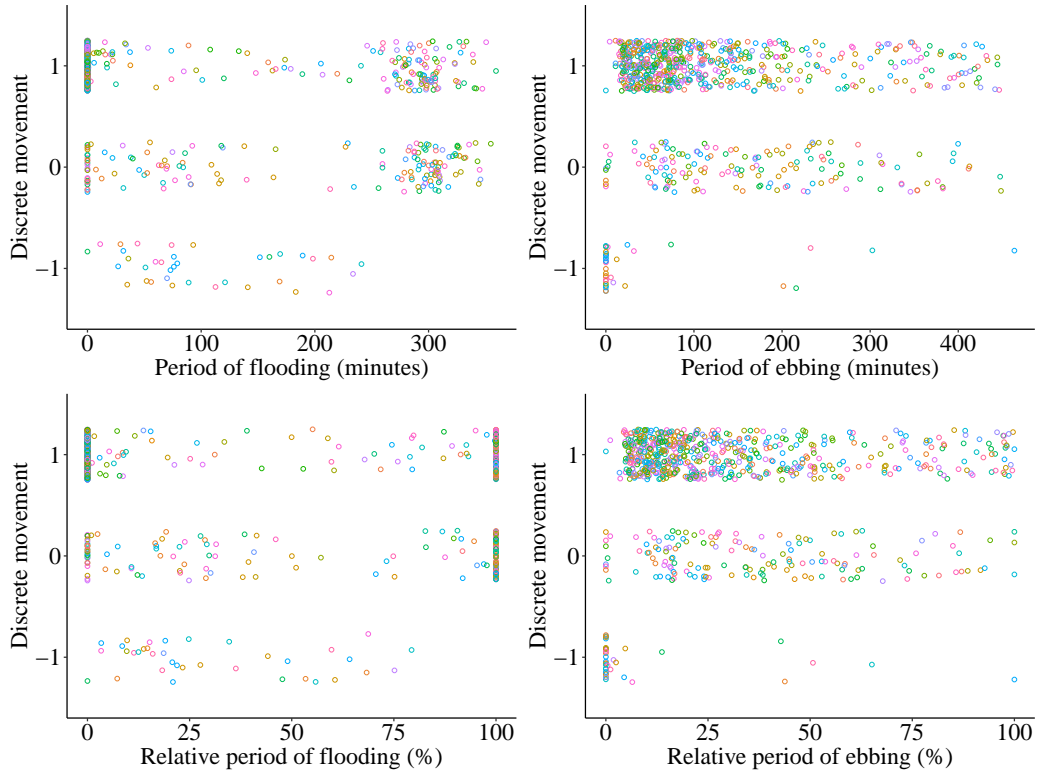


Figure 2: Graphs of discrete movement. Downstream movement (1); upstream movement (-1); residency (0) versus the relative (%) and actual (minutes) period of flooding and ebbing. All movement and residency intervals are depicted. Different colors represent different eels.

372 Transformed stacked density plots of swimming speed gave additional in-
 373 sights into the distribution of the data (Fig. 3). It is clear from these figures
 374 that the bimodal pattern in the data is the result of different tidal conditions
 375 rather than of individual differences. Most eels have swimming speeds rang-
 376 ing from 0 to 2 m s^{-1} , but swimming speeds from 0 to approximately 0.45 m
 377 s^{-1} typically occurred during pure flooding or a combination of flooding and
 378 ebbing, while swimming speeds of approximately 0.45 to 2 m s^{-1} typically

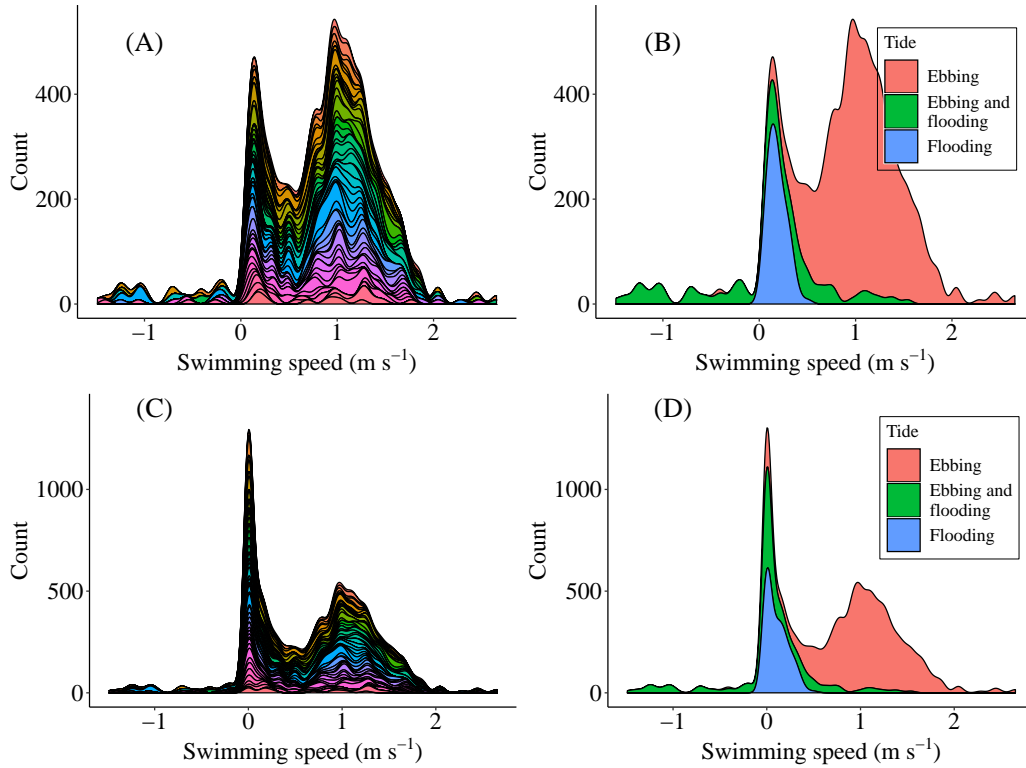


Figure 3: Transformed stacked density plots of eel swimming speed (m s^{-1}). To determine the count of the stacked density plots, the amount of movement (and residency) intervals for each swimming-speed-interval is divided by the width of a single swimming-speed interval (0.05 m s^{-1}). For example, in the swimming-speed interval centering the value 1 m s^{-1} , 25 intervals were found. Hence, 25 intervals divided by a width of 0.05 m s^{-1} yield a count of 500. In A and B the density plots of all movement intervals are given. The different colors in A depict the different eels, while the different colors in B depict whether movement intervals occurred during flooding, ebbing or a combination of both. In C and D the density plots of all residency intervals and movement intervals are given. The different colors in C depict the different eels, while the different colors in D depict whether residency and movement intervals occurred during flooding, ebbing or a combination of both.

379 occurred during pure ebbing events. This suggests that movement intervals
 380 with a swimming speed below approximately 0.45 m s^{-1} are likely to contain
 381 cryptic residencies, causing a delay in travel time.

Two-part and three-part models for passive telemetry data

Data	Model	RMSE
Original data set	One-part model	0.4165
	Two-part model: 0 vs not 0 m s ⁻¹	0.4073
	Selection model: 0 vs not 0 m s ⁻¹	0.4132
	Three-part model: 0 vs 0 vs 0 m s ⁻¹	0.4055
	Conditional inference random forests	0.3941
No upstream movement	One-part model	0.4051
	Two-part model: 0 vs not 0 m s ⁻¹	0.3804
	Selection model: 0 vs not 0 m s ⁻¹	0.5410
	Three-part model: 0 vs 0-0.45 vs 0.45-2.7 m s ⁻¹	0.3653
	Conditional inference random forests	0.3669

Table 1: RMSE values (Eq. 8) after Monte Carlo cross-validations (10^4 permutations) for different models and different data subsets.

382 *3.2. Model construction and evaluation*

383 For the original data set, Monte-Carlo cross-validations indicated that the
384 three-part model, which compartmentalized predictions into (1) residencies
385 and (2) downstream and (3) upstream movement, had the highest predic-
386 tive performance (RMSE = 0.4055), followed by the two-part model (RMSE
387 = 0.4073), which compartmentalized predictions in (1) residencies and (2)
388 movement, the selection model (RMSE = 0.4132) and the one-part model
389 (RMSE = 0.4165) (Table 1). After transformation of the upstream move-
390 ment intervals to residency intervals, Monte-Carlo cross-validations indicated
391 that the three-part model, which compartmentalized predictions into classes

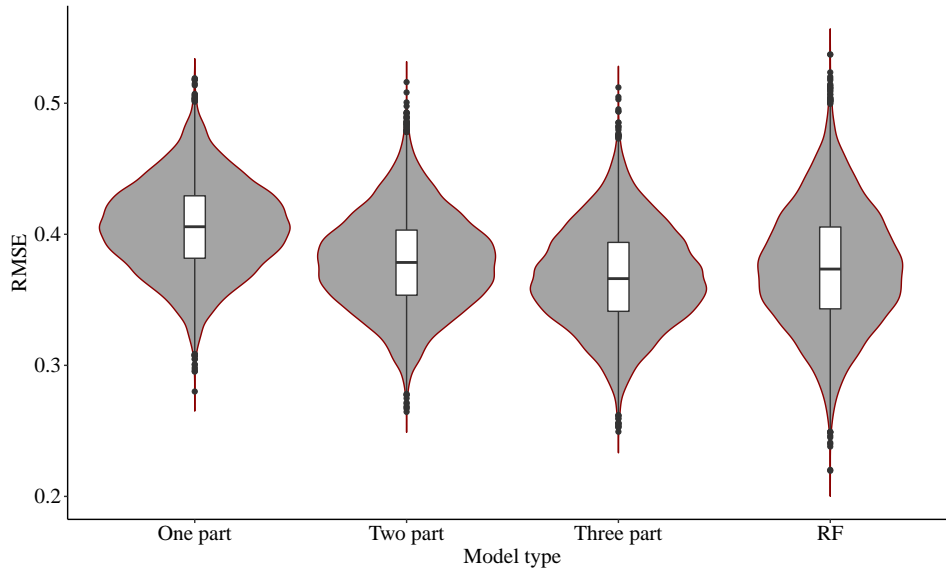


Figure 4: Violin plots representing the distribution of RMSE values obtained through cross-validation ($n=10^4$) for the different models. RMSE distributions are given for the one-part model, two-part model (0 vs not zero m s^{-1}), three-part model (0 vs 0-0.45 vs 0.45-2.7 m s^{-1}) and random forests model (RF). The data set without upstream intervals was used to construct the models.

392 of (1) 0, (2) 0 to 0.45 and (3) 0.45 to 2.7 m s^{-1} , had the highest predictive
 393 performance (RMSE = 0.3653) followed by the two-part model (RMSE =
 394 0.3804), which compartmentalized predictions into (1) residencies and (2)
 395 movement, one-part model (RMSE = 0.4051) and selection model (RMSE =
 396 0.5410) (Table 1). Since the three-part model performed best, it was retained
 397 for further analysis (Table 2).

398 The results of the multinomial model of the three-part model indicated
 399 that the distinction between <0.45 and >0.45 m s^{-1} was significantly better
 400 than the distinction between 0 and 0 to 0.45 m s^{-1} . The relative risk ratio
 401 for a one-percentage increase in the flood ratio was 0.987 for being between

Two-part and three-part models for passive telemetry data

			Intercept	Flood ratio	Distance	Moon phase	Tidal phase		
One-part model			Estimate	0.704	-0.0124	$4.94 \cdot 10^{-3}$	0.0885		
			CI	[0.629 0.780]	[-0.0133 -0.0116]	$[3.57 \cdot 10^{-3} \ 6.32 \cdot 10^{-3}]$	[0.0105 0.166]		
			p-value	0	0	0	0		
Two-part model	Binomial model			Estimate	2.68	-0.0464			
				CI	[2.37 3.03]	[-0.054 -0.0395]			
				p-value	0	0			
	Linear model			Estimate	0.795	-0.0137	$5.16 \cdot 10^{-3}$	0.0915	
				CI	[0.725 0.866]	[-0.0151 -0.0123]	$[3.90 \cdot 10^{-3} \ 6.43 \cdot 10^{-3}]$	[0.0101 0.174]	
				p-value	0	0	0	0.00258	
Three-part model	Multi-nomial model	0-0.45 vs 0 m s^{-1}			Estimate	0.507	-0.0134		
					CI	[0.0830 0.973]	[-0.0212 -0.00595]		
					p-value	0.105	$8.00 \cdot 10^{-4}$		
		0.45-2.7 vs 0 m s^{-1}			Estimate	2.96	-0.0987		
					CI	[2.57 3.43]	[-0.117 -0.0835]		
					p-value	0.126	0.00152		
	Gamma model	0-0.45 m s^{-1}			Estimate	-2.2	-0.00548	0.870	
					CI	[-3.31 -1.12]	[-0.00893 -0.00204]	[-0.192 1.94]	
					p-value	0.650	0.00167	0.648	
	Linear model	0.45-2.7 m s^{-1}			Estimate	0.82	-0.00455	$7.22 \cdot 10^{-3}$	0.0425
					CI	[0.750 0.889]	[-0.00690 -0.00219]	$[5.93 \cdot 10^{-3} \ 8.53 \cdot 10^{-3}]$	[-0.0436 0.127]
					p-value	$3.00 \cdot 10^{-4}$	0	0	0.0011

Table 2: Parameter estimates, 95% percentile confidence intervals (CI) and p-values of the one-part, two-part and three-part models obtained using a weighted bootstrap approach ($n=10^4$). The models had swimming speed as response and predictors were selected using a bootstrap selection procedure based on backwards elimination and AIC. The considered predictors were flood ratio (% percentage flood over total period), distance from source (km), moon phase (degree of moon illumination ranging from 0 to 1), tidal phase (ratio of the maximum difference in water level of the concerning day over the median of the maximum difference in water level per day of the entire study period) and day phase (categorical: day, night, dusk or dawn). The data set without upstream intervals was used to construct the models.

402 0 and 0.45 m s^{-1} versus 0 m s^{-1} and 0.907 for being between 0.45 and 2.7
403 m s^{-1} versus 0 m s^{-1} . The higher the flood ratio, the higher the probability
404 of an observed residency interval (0 m s^{-1}) and the lower the probability
405 of a movement interval with a swimming speed above 0.45 m s^{-1} . The
406 probability of a movement interval with a swimming speed below 0.45 m s^{-1}
407 s^{-1} shows an increasing trend with flood ratio similar to the probability of
408 residency intervals until a flood ratio of approximately 40% , after which the
409 probability decreases (Fig. 5).

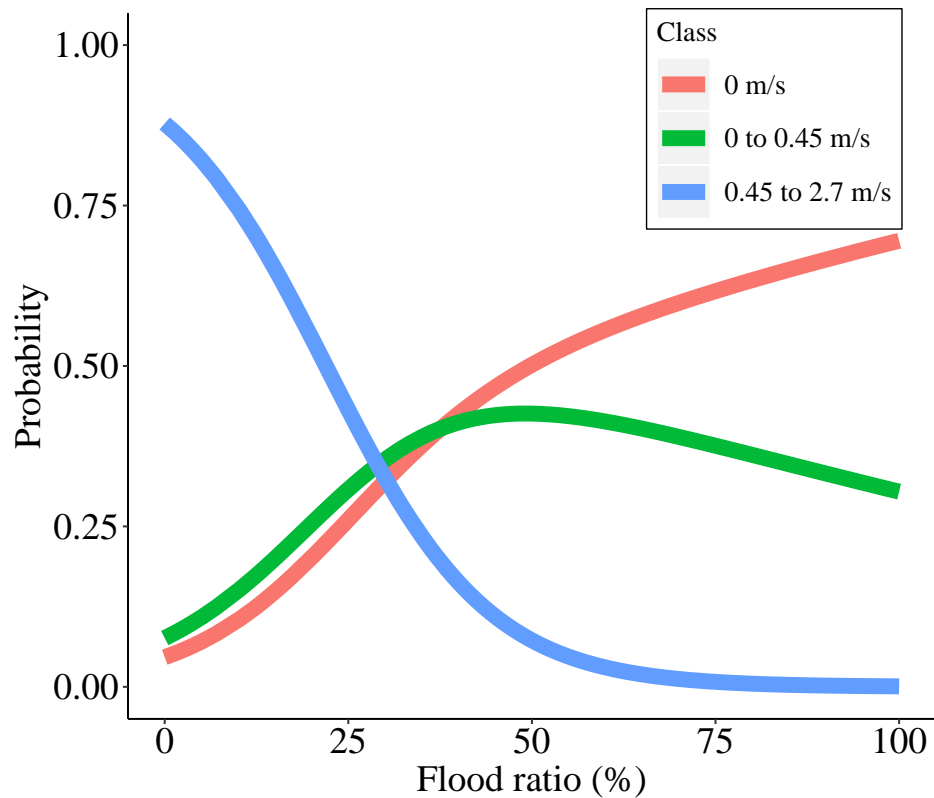


Figure 5: Output of the most parsimonious multinomial model with as response the three categories: 0, 0 to 0.45 , 0.45 to 2.7 m s^{-1} and as predictor the flood ratio. The probability of each class is given as a function of the flood ratio.

410 However, distinction between swimming speeds of 0 and 0 to 0.45 m s^{-1}
411 was necessary in order to fit a generalized linear model with gamma dis-
412 tribution through the data. Using a binomial model with contrasts <0.45
413 and $>0.45 \text{ m s}^{-1}$ followed by two linear models yielded a lower predictive
414 performance (RMSE = 0.3712) and would have violated model assumptions.
415 The multinomial model on its own provided a relatively low predictive per-
416 formance (RMSE=0.3940), but addition of a generalized linear model with
417 gamma distribution from 0 to 0.45 m s^{-1} and a linear model from 0.45 to
418 2.7 m s^{-1} increased the predictive performance with 7.3 % (RMSE=0.3653).
419 The gamma model from 0 to 0.45 m s^{-1} indicated a significant negative effect
420 of flood ratio. However, it should be noted that the model fit was relatively
421 poor as using a null model instead decreased the overall predictive perfor-
422 mance with only 1.1 % (RMSE = 0.3693). More benefit was gained from
423 the linear model for the part of 0.45 to 2.7 m s^{-1} as its omission reduced
424 overall predictive performance with 6.7 % (RMSE = 0.3898). The flood ra-
425 tio and moon phase had a significantly negative and positive effect on the
426 swimming speed, respectively, but were found to be far less important than
427 the significant positive effect of the distance to source. During ebbing tide,
428 eels closer to the North Sea had relatively higher swimming speeds. Finally,
429 all full model-parts of this three-part model were offered the variable eel ID
430 as fixed factor in the model selection process, but it was only retained in
431 the latter linear model from 0.45 to 2.7 m s^{-1} . This suggests that individual
432 differences were important to predict swimming speeds from 0.45 to 2.7 m

433 s^{-1} , but not to distinguish between classes (1) 0, (2) 0 to 0.45 and (3) 0.45
434 to 2.7 m s^{-1} or to predict the swimming speed from 0 to 0.45 m s^{-1} .

435 Similar predictors with reliable parameter estimates were retained in the
436 different models (Table 2). For the binomial part of the two-part models
437 only flood ratio was retained, while the one-part models and linear parts of
438 the two-part models retained, in order of decreasing importance, the factors
439 flood ratio, distance to source and moon phase. The variable importance
440 provided by the conditional inference random forests indicated that flood ra-
441 tio (0.3733) was most important, followed by distance from source (0.0609),
442 moon phase (0.0218), tidal phase (0.0204) and day phase (0.00796). The
443 conditional inference random forests performed better (2.8 %) than the best
444 statistical model when considering upstream movement intervals, but per-
445 formed slightly worse (0.4 %) than the best statistical model when upstream
446 movement intervals were not considered.

447 RMSE values of the one-part and two-part mixed models for the data
448 set without upstream movement intervals were 0.373 and 0.347 respectively.
449 Hence, the two-part mixed model explained patterns in the data 7.0 % better
450 than the one-part mixed model.

451 4. Discussion

452 4.1. Evaluating one-part, two-part and three-part (mixed) models

453 Movement decisions have been assessed in depth for a wide range of ani-
454 mals (Berdahl et al., 2017; Dechmann et al., 2017; O’Neal et al., 2018), but

455 the number of studies combining movement decisions with movement inten-
456 sity, e.g. swimming speed or distance covered, has been limited (Broder-
457 sen et al., 2008). Because zero values describe a unique behavioral aspect
458 in movement behavior, i.e. residencies, defining observed zeros and iden-
459 tifying cryptic zeros in telemetry data sets allowed to improve predictive
460 performance and to obtain more detailed ecological insights. The predictive
461 performances of the original three-part and two-part models were higher (be-
462 tween 2.2 and 9.8 %) than those of the one-part models, suggesting that the
463 conditions that affect the movement decision are not necessarily the same as
464 the conditions that affect the movement intensity. Taking into consideration
465 that both processes might be correlated did not improve predictions as the
466 selection models had a lower predictive performance. This is in concordance
467 with many econometric studies in which accounting for potential dependen-
468 cies between both parts of the model did not seem to add to the quality of
469 the predictions (Smith, 2003; Madden, 2008).

470 Although distinguishing between movement and residencies provided clearly
471 better predictions, further distinction between upstream and downstream
472 movement only provided marginally better predictive performances (0.4 %).
473 This might be because of the limited amount of upstream movement inter-
474 vals and the limited amount of individuals exhibiting upstream movement,
475 causing only a limited increase in explanatory power in the test set. How-
476 ever, the poor gain in explanatory power of the model may also be the result
477 of the similar conditions in which upstream movement and residencies oc-

478 curred. Indeed, considering upstream movement as residencies gone wrong,
479 resulted in a 6.6 % and 2.7 % increase in performance for the two-part and
480 one-part model respectively. This suggests that some eels are unsuccessful
481 in remaining resident during flooding as they are pushed back, or that they
482 mistake flooding for ebbing when moving along with the current. A final
483 improvement of model performance was apparent from further compartmenten-
484 talization. Distinction between swimming speeds of (1) 0, (2) 0 to 0.45 and
485 (3) 0.45 to 2.7 m s⁻¹ caused predictions of swimming speed to be 9.8 % bet-
486 ter. This model improvement was mainly the result of the contrasting tidal
487 conditions before and after 0.45 m s⁻¹, with eels facing or not facing a flood-
488 ing event respectively. Hence, compartmentalization was successful because
489 it adequately classified observed residencies (0 m s⁻¹), cryptic residencies (0
490 to 0.45 m s⁻¹) and movement intervals (0.45 to 2.7 m s⁻¹).

491 The results of the three-part model suggest that the movement decision
492 depends only on the tides, while the swimming speed is dependent on the
493 tides and the distance from source. The larger the contribution of flood, the
494 more likely a specific time lapse will be a residency interval rather than a
495 movement interval. In addition, eels which migrated during ebb tide and
496 which were already close to the sea, typically had the highest swimming
497 speed. The conditions during which the movement intervals of the first peak
498 of the bimodal pattern (<0.45 m s⁻¹) occurred were actually more closely
499 related to those of residency intervals than those of movement intervals of
500 the second peak of the bimodal pattern (>0.45 m s⁻¹). Within the ob-

501 served movement intervals characterized by a swimming speed below 0.45 m
502 s^{-1} , cryptic or undetected residencies were invoked by flooding events. Dur-
503 ing these flooding events, eels had to interrupt their journey, causing lower
504 observed swimming speeds. For swimming speeds above 0.45 m s^{-1} , the dis-
505 tance to the North Sea seemed to play a more important role than the tides.
506 In addition, individual variation was significantly more important for swim-
507 ming speeds above than below 0.45 m s^{-1} and also the movement decision
508 did not show any significant individual variation. This suggests that all eels
509 stay resident during flood, but also that some eels swim faster or slower than
510 others once the decision to continue their migration has been made. The
511 simple position estimates of a single individual would have made it difficult
512 to classify apparent non-movement as either (i) residencies or (ii) movement
513 without net gain in distance covered. However, the ability to quantify indi-
514 vidual variation from a large number of tagged individuals provided evidence
515 in favor of the first option. More specifically, as there were clearly faster
516 and slower swimming individuals, the second option would have resulted in
517 meaningful differences between individuals across all parts of the model (i.e.
518 some individuals would be pushed back while others would advance during
519 flood). This was, however, not the case.

520 One major advantage of telemetry is its ability to provide data on the
521 level of individuals, and therefore mixed models that account for individual
522 correlation are commonly used (Gillies et al., 2006; Hooten et al., 2017).
523 Two-part and three-part models can be easily extended to include mixed

524 effects in order to provide a higher explanatory power. In this study, the
525 explanatory power of mixed two-part models was 7.0 % higher than their one-
526 part equivalents. However, it should be noted that potential dependencies
527 between the elements of random and fixed factors across the different parts
528 were not considered. If correlation between the random effects across the
529 different parts is expected, a joint maximization of the likelihood functions
530 would be required. More research is needed to evaluate the added value of
531 such an approach as its importance is likely to be case-specific.

532 Eels have already been shown to exhibit selective tidal stream transport
533 (STST), as they make use of the tides to reach their destination with as little
534 energy expenditure as possible (Barry et al., 2016; Verhelst et al., 2018).
535 However, by comparing one-part with two-part and three-part models, we
536 illustrated that migrating fish exhibit complex behaviour and that models
537 initially constructed to assess human customer behavior, might also be of
538 use to study other animals (Farewell et al., 2017).

539 *4.2. Statistical models versus machine learning*

540 Statistical models are generally preferred over machine learning when the
541 number of available predictors is limited and the main purpose is to infer
542 ecological knowledge, while the contrary is true if predictive performance is
543 deemed more important than inference. Since researchers often seek to opti-
544 mize both knowledge and predictions, a mutually exclusive approach should
545 be avoided. In this study we started off with a simple linear regression (i.e.

546 one-part model), then moved further to a two-part model which combined a
547 binomial regression with linear regression, and finally ended up with a three-
548 part model which combined a multinomial model (via neural networks, i.e.
549 machine learning), generalized linear regression with gamma distribution and
550 linear regression. Because each step of the model improvement was supported
551 by ecological knowledge, i.e. being aware that the conditions that cause eels
552 to reside or to move might be different, and methodological considerations,
553 i.e. residencies taking place between gates are not directly observed but do
554 cause a travel delay, the final three-part model remained interpretable. The
555 conditional inference random forests provided similar results, though less in-
556 formative, and had only slightly higher or lower predictive performances than
557 the developed three-part models. Hence, appreciating the potential complex-
558 ity of animal behaviour and awareness towards the statistical framework that
559 machine learning algorithms are built upon, will provide researchers with the
560 best machine learning has to offer without compromising the lessons learnt
561 from statistical models.

562 *4.3. Recommendations for future studies*

563 In order for zero values to provide useful information, a good under-
564 standing of the meaning of zeros in the data is required. In this study we
565 considered all observed zeros to be true zeros, which is a plausible assumption
566 given the high detection probability of the network and mainly unidirectional
567 movement of migrating eel. In contrast, in case detection probabilities are

568 low, many zero values might actually be false zeros as the result of impor-
569 tant design and/or observer errors, and hence the probability of a false zero
570 should be explicitly integrated in the model. Since the detection probabilit-
571 ity is affected by the network design, transmission intervals and detection
572 range, which in turn is affected by environmental conditions (Reubens et al.,
573 2019b), an elaborate addition to the two-part models may be required to deal
574 with high levels of false zeros. In addition, a good understanding of the de-
575 tection range variability is also necessary to estimate any difference between
576 the observed and actual biological response. For instance, in this study, the
577 observed swimming speed of eel likely differed from the actual swimming
578 speed because of the unaccounted detection range variability. Furthermore,
579 the factors known to affect the detection range, i.e. tides (Mathies et al.,
580 2014), also seem to be affecting the movement behaviour of eel, introducing
581 not only noise but even a potential bias in the data. Independent range
582 tests at different locations along the estuary and at different moments within
583 the tidal cycle are a necessary addition to quantify the noise and/or bias
584 associated with detection range variability (Kessel et al., 2014).

585 It should also be noted that some limitations are inherent to the ap-
586 plied technique of passive telemetry and can only be resolved by additional
587 data collection. For example, when eels are between gates and there seem
588 to be travel delays during flood, apparent from reduced swimming speed,
589 it is difficult to tell whether eels (i) remained stationary near the bottom
590 to preserve energy or (ii) swam against the currents without much gain in

591 distance covered. Although the constructed models indicated that the first
592 option is much more likely than the second, depth profiles and actual swim-
593 ming speed measurements, obtained through archival tags with depth sensors
594 and accelerometers, would provide more direct estimates of specific animal
595 behavior and would allow to validate the results of this study.

596 **5. Conclusion**

597 In this study we illustrated how accounting for both well-defined and
598 cryptic residencies provides a better insight into the movement behaviour
599 of migrating eel. Two-part and three-part models turned out to be promis-
600 ing tools to deal with zero-inflated telemetry data, underlining the complex
601 behaviour of migrating fish. Nevertheless, a sound assessment of the detec-
602 tion range variability in combination with more fine-scale measurements of
603 environmental variables, is necessary in order to confirm the observed pat-
604 terns in eel movement and its relationship with environmental variables. Al-
605 though only data from one species, one telemetry network and one telemetry
606 technique was used, the proposed model framework can be used for study
607 cases with other species, networks and techniques (e.g. passive integrated
608 transponder and radio telemetry).

609 **Acknowledgements**

610 This work was supported by the Flemish branch of the LifeWatch ESFRI
611 observatory. P. Verhelst acknowledges the support of the Flemish Agency for

612 Innovation and Entrepreneurship (VLAIO), now under the auspices of the
613 National Science Fund FWO, during a large part of this study. R. Baeyens,
614 N. De Maerteleire, S. Franquet, E. Gelaude, T. Lanssens, S. Pieters, K.
615 Robberechts, T. Saerens, R. van der Speld, S. Vermeersch and Y. Verzelen
616 assisted with the data collection. B. Lonneville aided in the creation of the
617 map. This work makes use of data and infrastructure provided by VLIZ
618 and INBO and funded by Research Foundation - Flanders (FWO) as part
619 of the Belgian contribution to LifeWatch. We would also like to thank the
620 Royal Belgian Institute of Natural Sciences, Operational Directorate Natural
621 Environment (RHIB Tuimelaar) for infrastructure provision and Rijkswater-
622 staat (The Netherlands) for their cooperation and the permission to use their
623 marine buoys. This research has benefitted from a statistical consult with
624 Ghent University FIRE (Fostering Innovative Research based on Evidence)

625 **Authors' contributions**

626 S.B. conceived the ideas and designed methodology, analyzed the data
627 and led the writing of the manuscript; P.V., J.R. and S.B. collected the data;
628 All authors contributed critically to the drafts and gave final approval for
629 publication.

630 **6. References**

- 631 Arnold, G. P., Cook, P. H., 1984. Fish Migration by Selective Tidal Stream
632 Transport: First Results with a Computer Simulation Model for the Eu-
633 ropean Continental Shelf. In: McCleave, J. D., Arnold, G., Dodson, J. J.,
634 Neill, W. H. (Eds.), Mechanisms of Migration in Fishes. Springer, Boston,
635 pp. 227–261.
- 636 Austin, P. C., Tu, J. V., 2004. Bootstrap Methods for Developing Predictive
637 Models. *American Statistician* 58 (2), 131–137.
- 638 Barry, J., Newton, M., Dodd, J. A., Lucas, M. C., Boylan, P., Adams, C. E.,
639 2016. Freshwater and coastal migration patterns in the silver-stage eel
640 *Anguilla anguilla*. *Journal of Fish Biology* 88 (2), 676–689.
- 641 Belotti, F., Deb, P., Manning, W. G., Norton, E. C., 2015. twopm: Two-part
642 models. *Stata Journal* 15 (1), 3–20.
- 643 Berdahl, A., Westley, P. A., Quinn, T. P., 2017. Social interactions shape the
644 timing of spawning migrations in an anadromous fish. *Animal Behaviour*
645 126, 221–229.
- 646 Blasco-Moreno, A., Pérez-Casany, M., Puig, P., Morante, M., Castells, E.,
647 2019. What does a zero mean? Understanding false, random and structural
648 zeros in ecology. *Methods in Ecology and Evolution* 10, 949–959.
- 649 Breukelaar, A. W., Ingendahl, D., Vriese, F. T., De Laak, G., Staas, S.,
650 Klein Breteler, J. G. P., 2009. Route choices, migration speeds and daily

- 651 migration activity of European silver eels *Anguilla anguilla* in the River
652 Rhine, north-west Europe. *Journal of Fish Biology* 74 (9), 2139–2157.
- 653 Brodersen, J., Nilsson, P. A., Ammitzbøll, J., Hansson, L. A., Skov, C.,
654 Brönmark, C., 2008. Optimal swimming speed in head currents and effects
655 on distance movement of winter-migrating fish. *PLoS ONE* 3 (5), 1–7.
- 656 Brownscombe, J., Lédée, E., Graham, R., Struthers, D., Gutowsky, L. F. G.,
657 Nguyen, V. M., Young, N., Stokesbury, M. J. W., Holbrook, C. M., Bren-
658 den, T. O., Vandergoot, C. S., Murchie, K. J., Whoriskey, K., Mills, J.,
659 Steven, F., Krueger, C. C., Cooke, S. J., 2019. Conducting and interpret-
660 ing fish telemetry studies : considerations for researchers and resource
661 managers. *Reviews in Fish Biology and Fisheries* 29, 369–400.
- 662 Bruneel, S., Verhelst, P., Reubens, J., Baetens, J. M., Coeck, J., Moens, T.,
663 Goethals, P., 2020. Quantifying and reducing epistemic uncertainty of pas-
664 sive acoustic telemetry data from longitudinal aquatic systems. *Ecological*
665 *Informatics* 59.
- 666 Bultel, E., Lasne, E., Acou, A., Guillaudeau, J., Bertier, C., Feunteun, E.,
667 2014. Migration behaviour of silver eels (*Anguilla anguilla*) in a large estu-
668 ary of Western Europe inferred from acoustic telemetry. *Estuarine, Coastal*
669 *and Shelf Science* 137 (1), 23–31.
- 670 Bzdok, D., Altman, N., Krzywinski, M., 2018. Points of Significance: Statis-
671 tics versus machine learning. *Nature Methods* 15 (4), 233–234.

- 672 Cagua, E. F., Cochran, J. E. M., Rohner, C. A., Prebble, C. E. M., Sinclair-
673 taylor, T. H., Pierce, S. J., Berumen, M. L., 2015. Acoustic telemetry
674 reveals cryptic residency of whale sharks. *Biology letters* 11.
- 675 Cornet, E., Vereecken, H., Deschamps, M., Verwaest, T., Mostaert, F., 2016.
676 Hydrologisch jaarboek 2016. Tech. rep., Waterbouwkundig Laboratorium,
677 Antwerpen.
- 678 Davison, A. C., Hinkley, D. V., 1997. *Bootstrap Methods and their Applica-*
679 *tion*.
- 680 Deb, P., Holmes, A., 2002. Estimates of Use and Costs of Behavioural Health
681 Care: a comparison of Standard and Finite Mixture Models. In: Jones, A.,
682 O'Donnell, O. (Eds.), *Econometric Analysis of Health Data*. John Wiley
683 & Sons, Ch. 6.
- 684 Dechmann, D., Wikelski, M., Ellis-Soto, D., Safi, K., O'Mara, M., 2017. De-
685 terminants of spring migration departure decision in a bat. *Biology letters*
686 13 (9), 1–5.
- 687 Durif, C., Dufour, S., Elie, P., 4 2005. The silvering process of *Anguilla an-*
688 *guilla*: a new classification from the yellow resident to the silver migrating
689 stage. *Journal of Fish Biology* 66 (4), 1025–1043.
- 690 Farewell, V. T., Long, D. L., Tom, B. D. M., Yiu, S., Su, L., 2017. Two-Part
691 and Related Regression Models for Longitudinal Data. *Annual Review of*
692 *Statistics and Its Application* 4, 283–315.

- 693 Gillies, C. S., Hebblewhite, M., Nielsen, S. E., Krawchuk, M. E. G. A.,
694 Aldridge, C. L., Jacqueline, L., Saher, D. J., Stevens, C. E., Jerde, C. L.,
695 2006. Application of random effects to the study of resource selection by
696 animals. *Journal of Animal Ecology* 75, 887–898.
- 697 Glebe, B. D., Leggett, W. C., 1981. Temporal, Intra-population Differences
698 in Energy Allocation and Use by American Shad (*Alosa sapidissima*) Dur-
699 ing the Spawning Migration . *Canadian Journal of Fisheries and Aquatic*
700 *Sciences*.
- 701 Heckman, J., 1979. Sample Specification Bias as a Selection Error. *Econo-*
702 *metrica* 47, 153–161.
- 703 Hooten, M. B., Johnson, D. S., McClintock, B. T., Morales, J. M., 2017.
704 *Animal Movement: Statistical Models for Telemetry Data*, 1st Edition.
705 CRC Press.
- 706 Humphreys, B. R., 2013. *Dealing With Zeros in Economic Data*.
- 707 Joseph, J., Torney, C., Kings, M., Thornton, A., Madden, J., 2017. Applica-
708 tions of machine learning in animal behaviour studies. *Animal Behaviour*
709 124, 203–220.
- 710 Joseph, L. N., Conservancy, A. W., Elkin, C. M., Martin, T. G., 2009. Mod-
711 eling abundance using N-mixture models : The importance of considering
712 Modeling abundance using N -mixture models : the importance of consid-
713 ering ecological mechanisms (May 2019).

- 714 Kessel, S. T., Cooke, S. J., Heupel, M. R., Hussey, N. E., Simpfendorfer,
715 C. A., Vagle, S., Fisk, A. T., 2014. A review of detection range testing in
716 aquatic passive acoustic telemetry studies. *Reviews in Fish Biology and*
717 *Fisheries* 24 (1), 199–218.
- 718 Kraus, R. T., Holbrook, C. M., Vandergoot, C. S., Stewart, T. R., Faust,
719 M. D., Watkinson, D. A., Charles, C., Pegg, M., Enders, E. C., Krueger,
720 C. C., 2018. Evaluation of Acoustic Telemetry Grids for Determining
721 Aquatic Animal Movement and Survival. *Methods in Ecology and Evo-*
722 *lution*, 1–14.
- 723 Levy, Y., Plancke, Y., Peeters, P., Taverniers, E., Mostaert, F., 2014. Het
724 getij in de Zeeschelde en haar bijrivieren: langjarig overzicht van de voor-
725 naamste getijkarakteristieken. Tech. rep., Waterbouwkundig Laboratorium
726 (Antwerpen, België).
- 727 Madden, D., 2008. Sample selection versus two-part models revisited: The
728 case of female smoking and drinking. *Journal of Health Economics* 27 (2),
729 300–307.
- 730 Mathies, N. H., Ogburn, M. B., McFall, G., Fangman, S., 2014. Environ-
731 mental interference factors affecting detection range in acoustic telemetry
732 studies using fixed receiver arrays. *Marine Ecology Progress Series* 495,
733 27–38.
- 734 Melnychuk, M., 2012. Detection efficiency in telemetry studies: definitions

- 735 and evaluation methods. In: Adams, N., Beeman, J., Eiler, J. (Eds.),
736 Telemetry techniques: A user guide for fisheries research. American Fish-
737 eries Society, pp. 339–357.
- 738 Metcalfe, J. D., Arnold, G. P., Webb, P. W., 1990. The energetics of migration
739 by selective tidal stream transport: An analysis for plaice tracked in the
740 southern north sea. *Journal of the Marine Biological Association of the*
741 *United Kingdom*.
- 742 Neelon, B., O'Malley, A. J., Smith, V. A., 2016. Modeling zero-modified
743 count and semicontinuous data in health services research Part 1: back-
744 ground and overview. *Statistics in Medicine* 35 (27), 5070–5093.
- 745 O'Neal, B. J., Stafford, J. D., Larkin, R. P., Michel, E. S., 2018. The effect
746 of weather on the decision to migrate from stopover sites by autumn-
747 migrating ducks. *Movement Ecology* 6 (1), 1–9.
- 748 Perry, R. W., Castro-Santos, T., Holbrook, C. M., Sandford, B. P., 2012.
749 Using Mark-Recapture Models to Estimate Survival from Telemetry Data.
750 In: Adams, N., Beeman, J., Eiler, J. (Eds.), *Telemetry Techniques: A User*
751 *Guide for Fisheries Research*. American Fisheries Society, pp. 453–475.
- 752 Pohlmeier, W., Ulrich, V., 1995. An econometric model of the two-part de-
753 cisionmaking process in the demand for healthcare. *Journal of Human*
754 *Resources* 30 (2), 339–361.

- 755 Reubens, J., Verhelst, P., Knaap, I. V. D., Wydooghe, B., Milotic, T.,
756 Deneudt, K., Hernandez, F., Pauwels, I., 2019a. The need for aquatic
757 tracking networks : the Permanent Belgian Acoustic Receiver Network.
758 *Animal Biotelemetry* 7 (2), 1–6.
- 759 Reubens, J., Verhelst, P., van der Knaap, I., Deneudt, K., Moens, T., Hernan-
760 dez, F., 2019b. Environmental factors influence the detection probability
761 in acoustic telemetry in a marine environment: results from a new setup.
762 *Hydrobiologia* 845, 81–94.
- 763 Smith, M. D., 2003. On dependency in double-hurdle models. *Statistical*
764 *Papers* 44 (4), 581–595.
- 765 Steckenreuter, A., Hoenner, X., Huveneers, C., Simpfendorfer, C., Bus-
766 cot, M. J., Tattersall, K., Babcock, R., Heupel, M., Meekan, M., Van
767 Den Broek, J., McDowall, P., Peddemors, V., Harcourt, R., 2017. Opti-
768 mising the design of large-scale acoustic telemetry curtains. *Marine and*
769 *Freshwater Research* 68 (8), 1403–1413.
- 770 Thorstad, E. B., Rikardsen, A. H., Alp, A., Okland, F., 2013. The Use of
771 Electronic Tags in Fish Research - An Overview of Fish Telemetry Meth-
772 ods. *Turkish Journal of Fisheries and Aquatic Sciences* 13, 881–896.
- 773 Tukey, J. W., 1977. *Exploratory Data Analysis*. Pearson.
- 774 Verbiest, H., Breukelaar, A., Ovidio, M., Philippart, J. C., Belpaire, C., 2012.
775 Escapement success and patterns of downstream migration of female silver

- 776 eel *Anguilla anguilla* in the River Meuse. *Ecology of Freshwater Fish* 21 (3),
777 395–403.
- 778 Verhelst, P., Bruneel, S., Reubens, J., Coeck, J., Goethals, P., Oldoni, D.,
779 Moens, T., Mouton, A., 2018. Selective tidal stream transport in silver
780 European eel (*Anguilla anguilla* L.) – Migration behaviour in a dynamic
781 estuary. *Estuarine, Coastal and Shelf Science* 213, 260–268.
- 782 Wang, G., 2019. Machine learning for inferring animal behavior from location
783 and movement data. *Ecological Informatics* 49, 69–76.
- 784 Warton, D. I., 2005. Many zeros does not mean zero inflation: Comparing
785 the goodness-of-fit of parametric models to multivariate abundance data.
786 *Environmetrics* 16 (3), 275–289.
- 787 Whoriskey, K., Martins, E. G., Auger-Méthé, M., Gutowsky, L. F., Lennox,
788 R. J., Cooke, S. J., Power, M., Mills Flemming, J., 2019. Current and
789 emerging statistical techniques for aquatic telemetry data: A guide to
790 analysing spatially discrete animal detections. *Methods in Ecology and*
791 *Evolution* 10 (7), 935–948.
- 792 Zuur, A. F., Ieno, E. N., Walker, N. J., Saveliev, A. A., Smith, G. M.,
793 2009. *Mixed Effects Models and Extensions in Ecology with R*, 1st Edition.
794 Springer-Verlag New York, New York.

795 **Appendix A. Tagging procedure**

796 The following description is adopted from [Verhelst et al. \(2018\)](#). 100 Eels
797 were caught and tagged at the tidal weir in Merelbeke in the Zeeschelde dur-
798 ing late summer and autumn (September–November) of three consecutive
799 years (2015 till 2017) using double fyke nets. After periods of heavy rain,
800 water flows over the sluices allowing eels to swim over the sluices. Placing
801 the fyke nets behind the sluices and during periods of heavy rain, allowed to
802 coordinate capture events and improve the chance of capturing eel. Several
803 morphometric features were measured in order to determine the eel matura-
804 tion stage ([Durif et al., 2005](#)): Total length (TL, to the nearest mm), body
805 weight (W, to the nearest g), the vertical and horizontal eye diameter (EDv
806 and EDh respectively, to the nearest 0.01 mm) and the length of the pectoral
807 fin (FL, to the nearest 0.01 mm) (Table A.1). Only females were tagged, since
808 males are smaller than the minimum size handled in this study (< 450 mm
809 ([Durif et al., 2005](#))). Eels of three different maturation stages were tagged:
810 premigrant (F3, $n = 51$) and the two migrant stages F4 and F5 ($n = 21$ and
811 $n = 28$, respectively). The eels were tagged with V13 coded acoustic trans-
812 mitters (13 x 36 mm, weight in air 11 g, frequency 69 kHz, ping frequency:
813 60–100 s; estimated battery life: 1021-1219 days (battery life time depended
814 on specific transmitter settings), (Table A.2)) from VEMCO Ltd (Canada).
815 After anaesthetizing them with 0.3 ml/L clove oil, tags were implanted with
816 permanent monofilament ([Thorstad et al., 2013](#)). Eels recovered in a quar-
817 antine reservoir for approximately one hour and were subsequently released

818 at the nearest receiver.

Stage	Number	TL (mm)	BW (g)	EDh (mm)	EDv (mm)	FL (mm)
F3	51	702±57 (568 - 835)	674±165 (324 - 1106)	8.08±0.57 (6.77 - 9.08)	7.55±0.60 (6.20 - 9.70)	32.92±3.29 (26.76 - 40.32)
F4	21	810±57 (707 - 932)	1162±217 (771 - 1830)	10.41±0.92 (9.13 - 12.49)	9.66±0.78 (8.60 - 11.86)	40.86±4.32 (30.84 - 48.18)
F5	28	662±56 (575 - 775)	585±144 (417 - 912)	9.33±0.80 (8.14 - 11.18)	8.80±0.79 (7.62 - 10.39)	34.41±3.68 (28.97 - 45.37)

Table A.1: Number of all tagged female eels per stage with the different morphometrics: total length (TL), body weight (BW), horizontal and vertical eye diameters (EDh and EDv, respectively) and pectoral fin length (FL). Mean, standard deviation and range (between brackets) are indicated (Adopted from [Verhelst et al. \(2018\)](#)).

Number of transmitters	Step 1			Step 2			Battery life (days)
	PO	Ping frequency (s)	Duration (days)	PO	Ping frequency (s)	Duration (days)	
20	L	60 - 100	1216	NA	NA	NA	1216
40	H	60 - 100	120	L	60 - 100	901	1021
40	H	60 - 100	120	L	60 - 100	902	1022

Table A.2: The number and settings of the transmitters of all tagged eels per step: power output (PO; L = low power output, H = high power output), ping frequency (s) and the time duration (days) per step as well as the total battery life time (days). (Adopted from [Verhelst et al. \(2018\)](#))

819 **Appendix B. Telemetry network**

Two-part and three-part models for passive telemetry data

gate name	Distance (km)	Deployment date	Number of receivers	Receiver inactivity	Det. prob. (%)
s1	0.0	31/03/2015	1		100.0
s2	6.6	20/03/2016	1		100.0
s3	12.1	20/03/2016	1		97.1
s4	16.8	20/04/2015	1		97.4
s5	26.7	31/03/2015	1		99.1
s6	30.6	2/04/2015	1		98.7
s7	33.0	24/03/2016	1	17/10/2017 - 24/11/2017	96.7
s8	39.3	24/03/2016	1		81.6
s9	40.8	20/04/2015	1		99.9
s10	44.1	20/04/2015	1		99.3
s11	46.5	27/04/2015	1		100.0
s12	49.0	2/04/2015	1		98.4
s13	53.8	2/04/2015	1		93.2
s14	55.6	2/04/2015	1		100.0
s15	63.3	2/04/2015	2		100.0
s16	68.6	2/04/2015	2		100.0
s17	75.8	30/09/2015	3		100.0
s18	88.2	3/09/2015	2		77.8
ws1	112.8	22/09/2015	6		91.3

Table B.1: List of gates, with distance from Ghent (km), deployment date, number of included receivers, period of receiver inactivity and detection probability. Receiver inactivity represents the period during which one receiver of the gate was inactive. Adapted from [Bruneel et al. \(2020\)](#).

820 Appendix C. Figures

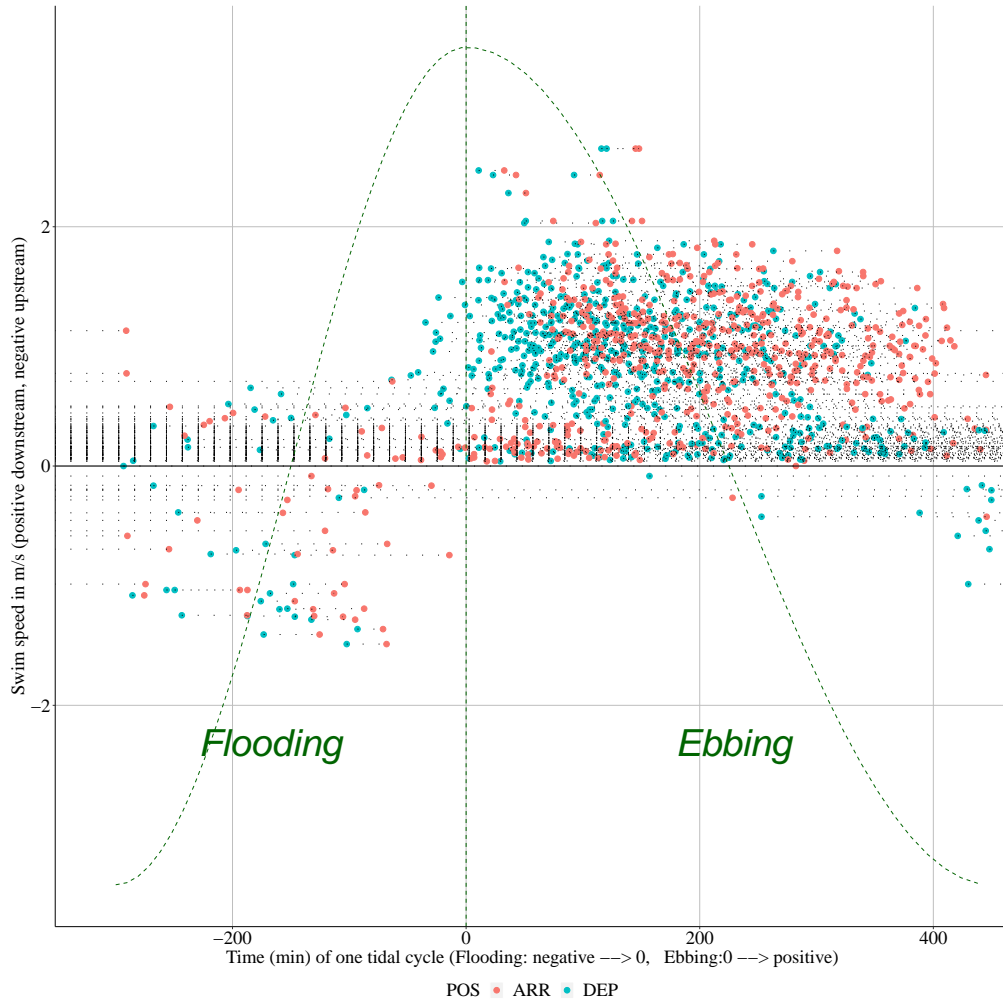


Figure C.1: Movement intervals of all tagged eels depicted by the departure (DEP) from a receiver and arrival (ARR) at another receiver. The swimming speed (m s^{-1}) during a movement interval is given in function of the moment within the tidal cycle. In the ZS, the period of ebbing is larger than the period of flooding, with differences being most pronounced upstream. However, for visualization purposes the average period of flooding (300 minutes) and period of ebbing (450 minutes) of the city of Dendermonde (in the center of the ZS) were used to rescale the TMIs (Levy et al., 2014)